HHS Public Access

Author manuscript

Magn Reson Med. Author manuscript; available in PMC 2021 September 16.

Published in final edited form as:

Magn Reson Med. 2021 August ; 86(2): 754–764. doi:10.1002/mrm.28743.

Time dependence in diffusion MRI predicts tissue outcome in ischemic stroke patients

Björn Lampinen[#1], **Jimmy Lätt**[#2], **Johan Wasselius**[3], **Danielle van Westen**[3], **Markus Nilsson**[3]

[1]Clinical Sciences Lund, Medical Radiation Physics, Lund University, Lund, Sweden

[2]Center for Medical Imaging and Physiology, Skåne University Hospital Lund, Lund, Sweden

[3]Clinical Sciences Lund, Radiology, Lund University, Lund, Sweden

[#] These authors contributed equally to this work.

Abstract

Purpose: Reperfusion therapy enables effective treatment of ischemic stroke presenting within 4–6 hours. However, tissue progression from ischemia to infarction is variable, and some patients benefit from treatment up until 24 hours. Improved imaging techniques are needed to identify these patients. Here, it was hypothesized that time dependence in diffusion MRI may predict tissue outcome in ischemic stroke.

Methods: Diffusion MRI data were acquired with multiple diffusion times in five non-reperfused patients at 2, 9, and 100 days after stroke onset. Maps of "rate of kurtosis change" (k), mean kurtosis, ADC, and fractional anisotropy were derived. The ADC maps defined lesions, normal-appearing tissue, and the lesion tissue that would either be infarcted or remain viable by day 100. Diffusion parameters were compared (1) between lesions and normal-appearing tissue, and (2) between lesion tissue that would be infarcted or remain viable.

Results: Positive values of k were observed within stroke lesions on day 2 ($P = .001$) and on day 9 ($P = .023$), indicating diffusional exchange. On day 100, high ADC values indicated infarction of 50 ± 20% of the lesion volumes. Tissue infarction was predicted by high k values both on day 2 ($P = .026$) and on day 9 ($P = .046$), by low mean kurtosis values on day 2 ($P = .043$), and by low fractional anisotropy values on day 9 ($P = .029$), but not by low ADC values.

Conclusions: Diffusion time dependence predicted tissue outcome in ischemic stroke more accurately than the ADC, and may be useful for predicting reperfusion benefit.

Keywords

diffusion-weighted imaging; human; ischemic stroke; reperfusion

Correspondence Björn Lampinen, Medical Radiation Physics, Barngatan 4, 221 85, Lund, Sweden. bjorn.lampinen@med.lu.se.

SUPPORTING INFORMATION

Additional Supporting Information may be found online in the Supporting Information section.

1 | INTRODUCTION

Reperfusion therapy with intravenous tissue plasminogen activator or endovascular thrombectomy enables effective treatment of patients presenting within 4–6 hours of ischemic stroke.[1-4] However, the ability to salvage brain tissue depends not only on the duration of hypoperfusion but also on its effect on tissue, which depends on individual factors such as collateral supply.[5-7] Accordingly, some patients benefit from reperfusion even up to 16–24 hours following stroke onset.[8,9] Individualized assessment of reperfusion benefit is therefore needed to avoid missed treatment opportunities.[6,7,10,11]

Many imaging techniques have been proposed for identifying patients who are likely to benefit from reperfusion therapy following ischemic stroke. Typically, perfusion imaging is used to define tissue at risk of infarction. Diffusion MRI (dMRI) is then used to define tissue that cannot be salvaged by reperfusion (ischemic core) by detecting a reduction in the apparent diffusion coefficient (ADC). This “diffusion-perfusion mismatch” has been suggested as a method of defining the volume of salvageable tissue (ischemic penumbra).[8,9,12,13] However, the transfer of these techniques into clinical practice has been slow,[14] and there are issues concerning reliability. Quantitative perfusion imaging is challenging, and the threshold between penumbra and benign oligemia varies across tissue and may change over time.[10,11,15,16] Although ADC reduction is sensitive to critical hypoperfusion, it detects tissue with very heterogeneous damage[17-19] and that may survive either with or without reperfusion.[20-24] Thus, improved imaging techniques are needed for the prediction of reperfusion benefit.

Diffusion MRI can provide more information on tissue microstructure and the ischemic process than what is conveyed by the ADC alone. The ADC captures the initial slope of the diffusion-weighted signal at low b-values and reflects the *average* diffusivity within a multitude of microscopic environments.[25] The *variance* in diffusivities across those environments is probed by the mean kurtosis (MK) from diffusion kurtosis imaging, which captures the signal curvature observed at higher b-values.[26] The MK is elevated within ischemic stroke lesions,[27] and to consider MK elevation in addition to ADC reduction may yield a more accurate definition of ischemic core.[28,29] Moreover, ischemic stroke is associated with a diffusion time dependence of both the ADC and the MK. For example, the ADC reduction in ischemic stroke is reversed for very short diffusion times.[30] Conversely, effects of diffusional exchange have been demonstrated for very long diffusion times, in which the MK is reduced from exchange-driven mixing of water between microscopic environments.[31] Thus, diffusion time dependence appears tightly linked to the ischemic process. However, the relationship between diffusion time dependence and the outcome of ischemic tissue has, to our knowledge, not yet been investigated.

This study followed a small cohort of patients from the subacute to the chronic stage of ischemic stroke using repeated dMRI examinations with multiple diffusion times. We hypothesize that assessment of diffusion time dependence may predict tissue outcome in ischemic stroke, and may be useful for predicting reperfusion benefit. To test this hypothesis, we estimate the “rate of kurtosis change” (k) within stroke lesions at the

subacute stage, and compare this parameter between the lesion tissue that would either be infarcted or remain viable by the chronic stage.

2 | METHODS

2.1 | Patients and study design

The study followed patients at three time points after ischemic stroke onset using dMRI of the brain. Patients were recruited from the Department of Neurology at Skåne University Hospital, Lund, Sweden. The inclusion criteria were (1) ischemic stroke with a known time of onset, (2) no reperfusion therapy given, (3) a (largest) lesion diameter of at least 3 cm, (4) an established region of ADC reduction at the first imaging time point, and (5) the ability and willingness of the patient to complete 3 months of follow-up.

Five acute stroke patients met the inclusion criteria (Table 1): 3 females and 2 males with an age of 47 ± 10 years (mean ± SD) at the first examination. All patients underwent dMRI 1–4 days following stroke onset, representing the early subacute stage when the volume of ADC reduction should be near fully developed; 8–11 days following stroke onset, representing the late subacute stage when the ADC should be pseudo-normalized; and 95–133 days following stroke onset, representing the chronic stage when the final infarction volume should be fully developed. Mean duration from stroke onset was 2, 9, and 111 days for the three imaging time points, which are henceforth referred to as “day 2,” “day 9,” and “day 100,” respectively. The lesions were heterogenic, originating from occlusions of different branches of the medial and posterior cerebral arteries.

The study was approved by the Swedish Ethical Review Authority, and all patients gave written informed consent according to recommendations of the Declaration of Helsinki.

2.2 | MRI acquisition

Magnetic resonance imaging acquisition of the brain was performed on an Achieva 3T system (Philips, Best, the Netherlands). dMRI data were acquired with a diffusion-weighted EPI sequence, using $b = 0.2$ and $b = 0.5, 1.0, \ldots, 4.0$ ms/μm^2, each repeated over six directions and two diffusion times: $T_D = 30$ ms and $T_D = 60$ ms. The diffusion-encoding gradient duration was fixed at $\delta = 21$ ms. Other sequence parameters were TR = 2000 ms, TE = 105 ms, FOV = 23 × 23 cm^2, 2 × 2 mm^2 in-plane resolution, five 4 mm thick slices placed over the lesion, parallel imaging factor 2 (SENSE), partial Fourier factor 0.8, bandwidth = 2960 Hz/pixel, and an acquisition time of 12 minutes.

2.3 | MRI post-processing

The dMRI data were corrected for eddy currents and subject motion using ElastiX[32] with extrapolated target volumes.[33] The corrected data were arithmetically averaged across the diffusion-encoding directions for each b-value and each diffusion time. The image volumes from each time point were spatially aligned to a common reference space (the day 2 image) using ElastiX and rigid-body transformations between the $b = 0.2$ ms/μm^2 images. To correct for differences in signal gain between diffusion times, the signal was normalized

with respect to the $b = 0.2$ ms/μm^2 images. Finally, the data were smoothed using a 3D Gaussian kernel with a SD of 1 × 1 × 2 mm^3.

2.4 | Signal modeling and parameter maps

To assess diffusion time dependence, the dMRI data were analyzed with the signal expression proposed by Ning et al,[34] according to

$$\log(S) \approx \log(S_0) - b\,\mathrm{ADC} + b^2\,\mathrm{MK}\,(1 - \Gamma k)\,\mathrm{ADC}^2 / 6, \quad (1)$$

where S_0 is the non-diffusion-weighted signal; MK is the mean kurtosis in the absence of time dependence; and k is the rate of kurtosis change. For a single diffusion-encoding sequence, the exchange-weighting time Γ is given by

$$\Gamma = 1/3\,(\Delta^3 - \Delta^2\delta + 2/3\,\delta^2\Delta - 4/21\,\delta^3)\;/\;(\Delta - 1/3\,\delta)^2, \quad (2)$$

where δ and Δ are the duration and separation of the leading edges of the diffusion-encoding gradients, respectively, and are related to the diffusion time according to $T_D = \Delta - 1/3\,\delta$. Notably, $\Gamma \approx T_D/3$ when $\Delta >> \delta$.

Equation 1 is derived from a cumulant expansion of the two-compartment Kärger model with exchange, in which the k parameter is the exchange rate.[34,35] In the absence of restricted diffusion, k should be positive and reflect diffusional exchange similar to the apparent exchange rate parameter from filter exchange imaging.[34,36-39] However, restricted diffusion has been demonstrated in ischemic stroke,[30] which could result in negative values of k. More generally, k reflects time dependence of the diffusional kurtosis, where exchange effects will increase k and reduce kurtosis and where restricted diffusion will have the opposite effect.[40] Thus, in this work, k is referred to as the rate of kurtosis change. Note that restricted diffusion refers to effects of barriers on the temporal evolution of the diffusion process rather than a *reduced* diffusion as in a low ADC. Finally, note that we applied Equation 1 to direction-averaged data, which assumes that effects of diffusion anisotropy can be neglected. The MK estimated from direction-averaged data differs from the MK obtained from diffusion kurtosis imaging unless diffusion is completely isotropic. More generally, it corresponds to the $\mathrm{MK_T}$ parameter as defined in the context of tensor-valued diffusion encoding.[41-44]

To obtain maps of k, ADC and MK, Equation 1 was fitted to the dMRI data voxel-by-voxel using linear regression with heteroscedasticity correction. The fitting excluded data points with signal values equal to or below zero. To obtain maps of the fractional anisotropy (FA), a DTI analysis[45] was performed for the data acquired with $T_D = 30$ ms and $b \leq 1.0$ ms/μm^2.

2.5 | Regions of interest

As a basis for all investigations, regions of interest (ROIs) defining stroke lesions and normal-appearing brain tissue were determined on the spatially aligned ADC maps of each patient (Figure 1). The manual review was performed by B.L. together with D.v.W., a senior neuroradiologist, and the automatic steps were performed using MATLAB (R2015b; MathWorks, Natick, MA).

To define the full lesion volumes, ROIs were manually determined in the ADC maps on day 2, where the lesions stood out as dark regions with sharp borders to the surrounding tissue (Figure 1). These ROIs were then used to define the lesion volumes for day 9 and day 100, but with small manual corrections for tissue displacement and EPI-related distortions. The corrections were guided by morphological correspondence in the S_0 and FA maps without considering the maps of k.

To define the lesion tissue that would be infarcted by day 100, "infarction" ROIs were created by applying the full lesion volume ROIs to the day 100 ADC maps and selecting the enclosed voxels with ADC > 1.2 μm^2/ms (Figure 1). These infarction ROIs were then applied to the day 2 and day 9 maps to define the tissue that would later become infarcted. Again, small manual corrections were made as described previously. The lesion tissue that would remain viable was then defined, for each time point, by "viable" ROIs determined from the difference between the full lesion ROIs and the infarction ROIs.

To define normal-appearing brain tissue, ROIs were determined for each time point by taking whole-brain masks (based on thresholding of the S_0 maps) and from these subtracting the full lesion ROIs, voxels adjacent to lesions, and voxels with ADC > 1.2 μm^2/ms (Figure 1).

2.6 | Diffusion time dependence versus tissue outcome

Two approaches were used to investigate whether assessment of diffusion time dependence may predict tissue outcome in ischemic stroke. First, we studied the progression of k by comparing lesions with normal-appearing tissue. Second, we tested whether k at the two subacute time points differed between the lesion tissue that would become infarcted and the lesion tissue that would remain viable. For reference, the comparisons were also performed for the ADC, MK, and FA.

2.7 | Statistical analysis

The comparisons were based on average parameter values obtained by applying ROIs to the fitted maps and computing the mean value of the enclosed voxels. To reduce the effect of imaging artifacts, the means ignored the upper and lower half percentiles. For each time point, paired t-tests compared the average values of k, ADC, MK, and FA between the ROIs representing the full lesion volumes and normal-appearing tissue. For day 2 and day 9, paired t-tests compared the average values of each parameter between the ROIs representing lesion tissue that would be infarcted by day 100 and lesion tissue that would remain viable. Two-sided $P < .05$ was considered significant for all tests. Continuous variables are presented with mean and inter-patient SD.

3 | RESULTS

3.1 | Demonstration of diffusion time dependence in ischemic stroke

Figure 2A demonstrates diffusion time dependence in a brain region featuring ADC reduction and diffusion-weighted image hyperintensity on day 2. The lesion was salient in the k map, where it featured bright coherent regions with high values against a noisy-

appearing background. Figure 2B demonstrates how the intensity in the k map reflected a diffusion time (T_D) dependence of the dMRI signal. Where the k map was bright with positive values (i), a prolonged T_D yielded a decreased signal curvature at high b-values and a reduced effective diffusional kurtosis (Equation 1). This indicates diffusional exchange.[40] Where the k map was dark with negative values (ii), a prolonged T_D had the opposite effect on the signal, which indicates restricted diffusion.[40] Where k was near zero (iii), the signal overlapped for the two different diffusion times, indicating no diffusion time dependence.

3.2 | Diffusion time dependence in lesions versus in normal-appearing tissue

Figure 3 shows the progression of the k map for an example stroke lesion through the subacute stage (day 2 and day 9) to the chronic stage (day 100), together with maps of the ADC, MK, and FA. Corresponding figures are presented for all lesions in Supporting Information Figures S1-S5. Table 2 provides the average parameter values at each time point and reports any statistical differences between lesions and normal-appearing tissue.

On day 2, in the lesions of all 5 patients, the k maps featured large bright regions indicating elevated rates of water exchange together with smaller darker regions indicating restricted diffusion or no time dependence (example in Figure 3). On day 9, in 3 out of 5 patients, a weaker but similar pattern of elevated k was observed (Figure 4). The k values were higher within the lesions than within the normal-appearing tissue, particularly on day 2 (Table 2; $6.0 \pm 1.2\ s^{-1}$ vs $2.5 \pm 0.8\ s^{-1}$; mean ± SD; $P = .001$) but also on day 9 ($5.0 \pm 1.5\ s^{-1}$ vs $2.0 \pm 1.3\ s^{-1}$; $P = .023$). Diffusion time dependence was mostly absent on day 100 ($-0.6 \pm 1.4\ s^{-1}$ vs $2.0 \pm 1.8\ s^{-1}$; $P = .073$).

The ADC within the lesions progressed from reduced (day 2) to pseudo-normalized (day 9) during the subacute stage, to elevated by the chronic stage (day 100; Figure 3 and Table 2). The ADC elevation on day 100 was heterogeneous within the lesions. Some regions were very bright, indicating liquefaction and infarcted tissue, whereas others were similar to normal-appearing tissue, indicating viable tissue. Viable tissue was observed at the chronic stage for all 5 patients (Figure 4), indicating infarction of 50 ± 20% of the lesion volumes. No infarcted tissue was observed outside the original volumes of ADC reduction.

The MK within the lesions was elevated at the subacute stage, and transitioned to reduced by the chronic stage (Figure 3 and Table 2). The FA within the lesions was similar at all time points and lower than in normal-appearing tissue.

3.3 | Diffusion time dependence versus tissue outcome

Figure 4 compares the k maps of all stroke lesions at both subacute time points (day 2 and 9) with the ADC maps at the chronic stage. Table 3 compares the average k on day 2 and on day 9 between lesion tissue that would have different outcomes (infarcted vs viable), repeated for the ADC, MK, and FA.

The pattern of elevated k within the lesions at the subacute stage appeared to coincide with the pattern of elevated ADC at the chronic stage (Figure 4), thus indicating a relationship between elevated diffusional exchange and eventual infarction. The values of k were higher within the lesion tissue that would become infarcted by day 100 than in the lesion tissue that

would remain viable, both on day 2 (Table 3; 9.5 ± 3.1 s^{-1} vs 3.6 ± 3.0 s^{-1}; mean ± SD, P = .026) and on day 9 (7.2 ± 3.4 s^{-1} vs 3.6 ± 1.0 s^{-1}; P = .046). Tissue that would become infarcted also exhibited lower MK values on day 2 (P = .043), and lower FA values on day 9 (P = .029). No relationship was observed between ADC at the subacute stage and tissue outcome.

4 | DISCUSSION

The results show that diffusion time dependence in the early stage of ischemic stroke may predict tissue outcome in the late stage, and may therefore be useful for predicting reperfusion benefit. On day 100, only approximately half of the original volumes of ADC reduction showed signs of infarction. High k values on both day 2 and day 9 were predictive of this infarction, whereas low ADC values were not. Thus, the use of diffusion time dependence improved the definition of ischemic core. The dMRI technique used in this study is vendor-independent, and an implementation optimized for clinical routine imaging should require only a few minutes of extra scan time.

The eventual infarction of only part of the tissue that exhibited ADC reduction on day 2 is consistent with previous results in non-reperfused ischemic stroke,[21,22] and demonstrates that ADC reduction is sensitive but not specific to critical hypoperfusion. The reduced water mobility in ischemic stroke has been related to “beading” of axons and dendrites, as water follows osmotic gradients into the intracellular space and causes cellular swelling.[30,46-49] The ADC reduction occurs within minutes in tissue where perfusion falls below the threshold of adenosine-5′-triphosphate depletion, and then occurs at progressively later time points in tissue with higher perfusion levels,[50] which gives the impression of an expanding infarction. The reduction does not imply infarction, however. Within 2 hours after vascular occlusion, ADC reduction also occurs in reversibly ischemic tissue.[50] Furthermore, the value of the reduced ADC reflects the tissue composition rather than the degree of tissue damage.[17-20,51,52] Hence, ADC reduction in ischemic stroke appears to reflect the microstructural consequences of a certain level of hypoperfusion without providing further information on actual tissue damage.

The high values of k within the lesions confirm the presence of elevated rates of water exchange in subacute ischemic stroke (Table 2).[31] The k elevation was more related to tissue outcome than the ADC reduction (Table 3) and also persisted longer (Figure 3, day 9). This suggests that rather than reflecting reversible cellular swelling in the early stages of ischemic cell death, as the ADC reduction, the elevated rates of water exchange may reflect membrane damage and increased cellular permeability in the later stages.[53,54] In ischemic cardiomyocytes, the progression toward necrosis is characterized by accumulation of damage to the plasma membrane through, for example, phospholipid depletion, oxidative stress, pore formation, and an unbalanced fatty acid metabolism that alters fluidity.[53,55] Apart from such mechanisms, elevated rates of water exchange may reflect an increased expression of membrane channels.[56] In ischemic stroke, large and supposedly water-permeable volume-regulated anion channels are thought to be active participants in the process of excitotoxicity, which expands the infarction into penumbral tissue.[46,57,58] Thus, we hypothesize that elevated rates of water exchange in ischemic

stroke reflects tissue damage and increased membrane permeability within the developing infarction.

We identified six main limitations to this study. First, the patient material was small and heterogeneous with respect to lesion types and exact imaging time points (Table 1), which limited the statistical power. Furthermore, the patients were not imaged earlier than approximately 2 days after stroke onset. Although this was adequate for investigating diffusion time dependence within volumes of developed ADC reduction, data acquired at earlier time points would be necessary to directly study the utility of diffusion time dependence for predicting reperfusion benefit. Second, data featured large voxels, low spatial coverage, and lacked reversed-polarity phase encoding for correction of susceptibility-induced distortions.[59] This made spatial alignment of the images challenging and may have affected the accuracy of following tissue longitudinally using ROIs. The main finding of diffusion time dependence in ischemic stroke and its relationship with tissue outcome should be robust to this limitation, however, as it was apparent even on the single-patient level (Figure 4). Third, due to these limitations, gray and white matter were not analyzed separately. Diffusional exchange may be affected by myelin content,[60,61] and the importance of tissue composition on interpreting k should be explored in future studies. In this study, the relationships between a low MK and a low FA with infarction (Table 3) could reflect a gray matter focus of these particular lesions. The FA result is consistent with Jin et al,[62] but the MK result is opposite to the findings in white matter by Cheung et al[28] and by Yin et al,[29] obtained without considering time dependence. Fourth, the acquisition used only six independent directions, which may have been insufficient for a rotationally invariant arithmetic average at high b-values.[63] This may have increased the parameter variance but should not have biased the results, which were based on large ROI averages. Fifth, the effects of Rician noise may have been non-negligible at our rather high b-values. This may have introduced a negative bias on k on the order of 25%, assuming an SNR of 40 at $b = 0$ ms/μm^2 (Supporting Information Figure S6). Future studies should address this limitation by using, for example, better head coils, compressed sensing,[64] denoising,[65] or super-resolution techniques.[66] Sixth, the signal model (Equation 1) features assumptions that can be sources of bias. In particular, Equation 1 assumes Gaussian diffusion within each microscopic environment.[34] This was not valid for our data, which exhibited effects of restricted diffusion (Figure 2), consistent with previous results in ischemic stroke obtained using much shorter diffusion times.[30] This entanglement affected the k parameter, resulting in negative values, a reduced specificity to exchange, and a reduced sensitivity to time dependence. It is now known how to disentangle the effects of exchange and restricted diffusion,[67] but that theory was not available at the time of the study and the data acquisition was not adjusted accordingly. An alternative means to obtain specificity to exchange is to acquire data with double diffusion encoding, as in the filter exchange imaging approach.[36-39] Furthermore, the linear relationship with k in Equation 1 assumes $\Gamma k << 1$,[34] which may yield a negative bias when k is large (Supporting Information Figure S6). A more exact non-linear expression has been presented by Jensen and Helpern.[68] Thus, the herein used k parameter should be seen as a means of capturing time dependence whose interpretation in terms of specific physical quantities such as membrane permeability requires additional assumptions. The biophysical

meaning of diffusion time dependence in ischemic stroke needs to be explored further using more modern approaches to data acquisition and modeling.

5 | CONCLUSIONS

Assessment of diffusion time dependence is potentially useful for predicting reperfusion benefit in ischemic stroke patients. Here, diffusion time dependence provided increased specificity to tissue infarction, and therefore ischemic core. Future studies should investigate whether assessment of diffusion time dependence may improve the differentiation of ischemic penumbra and benign oligemia, such as through sensitivity to water exchange associated with excitotoxicity, which is dependent on water-permeable ion channels. Future studies should also include more patients, use more modern approaches to data acquisition and analysis, and consider including independent techniques such as PET,[19] spectroscopy imaging,[18] or histology,[17] to validate diffusion time dependence as a marker of tissue damage in ischemic stroke.

Supplementary Material

Refer to Web version on PubMed Central for supplementary material.

ACKNOWLEDGMENT

The authors thank Philips Healthcare for providing access to the pulse programming environment and Lee Nolan for language editing.

Funding information

Swedish Research Council (2016-03443) and the National Institutes of Health (P41EB015902 and R01MH074794)

DATA AVAILABILITY STATEMENT

All post-processing, signal modeling, and statistical analysis were performed using MATLAB and ElastiX. Model fitting used the multidimensional dMRI toolbox,[69] available at https://github.com/belampinen/md-dmri.

REFERENCES

1. Lees K, Bluhmki E, Von Kummer R, et al.Time to treatment with intravenous alteplase and outcome in stroke: an updated pooled analysis of ECASS, ATLANTIS, NINDS, and EPITHET trials. Lancet. 2010;375:1695–1703. [PubMed: 20472172]
2. Emberson J, Lees KR, Lyden P, et al.Effect of treatment delay, age, and stroke severity on the effects of intravenous thrombolysis with alteplase for acute ischaemic stroke: a meta-analysis of individual patient data from randomised trials. Lancet. 2014;384:1929–1935. [PubMed: 25106063]
3. Goyal M, Menon BK, van Zwam WH, et al.Endovascular thrombectomy after large-vessel ischaemic stroke: a meta-analysis of individual patient data from five randomised trials. Lancet. 2016;387:1723–1731. [PubMed: 26898852]
4. Saver JL, Goyal M, Van der Lugt A, et al.Time to treatment with endovascular thrombectomy and outcomes from ischemic stroke: a meta-analysis. JAMA. 2016;316:1279–1289. [PubMed: 27673305]

5. Wheeler HM, Mlynash M, Inoue M, et al.The growth rate of early DWI lesions is highly variable and associated with penumbral salvage and clinical outcomes following endovascular reperfusion. Int J Stroke. 2015;10:723–729. [PubMed: 25580662]

6. Rocha M, Jovin TGJS. Fast versus slow progressors of infarct growth in large vessel occlusion stroke: clinical and research implications. Stroke. 2017;48:2621–2627. [PubMed: 28794271]

7. Albers GW. Late window paradox. Stroke. 2018;49:768–771. [PubMed: 29367336]

8. Albers GW, Marks MP, Kemp S, et al.Thrombectomy for stroke at 6 to 16 hours with selection by perfusion imaging. N Engl J Med. 2018;378:708–718. [PubMed: 29364767]

9. Nogueira RG, Jadhav AP, Haussen DC, et al.Thrombectomy 6 to 24 hours after stroke with a mismatch between deficit and infarct. N Engl J Med. 2018;378:11–21. [PubMed: 29129157]

10. Yuh WT, Alexander MD, Ueda T, et al.Revisiting current golden rules in managing acute ischemic stroke: evaluation of new strategies to further improve treatment selection and outcome. Am J Roentgenol. 2017;208:32–41. [PubMed: 27681054]

11. Leigh R, Knutsson L, Zhou J, van Zijl PC. Imaging the physiological evolution of the ischemic penumbra in acute ischemic stroke. J Cerebr Blood Flow Metab. 2018;38:1500–1516.

12. Albers GW. Expanding the window for thrombolytic therapy in acute stroke: the potential role of acute MRI for patient selection. Stroke. 1999;30:2230–2237. [PubMed: 10512933]

13. Lansberg MG, Straka M, Kemp S, et al.MRI profile and response to endovascular reperfusion after stroke (DEFUSE 2): a prospective cohort study. Lancet Neurol. 2012;11:860–867. [PubMed: 22954705]

14. Powers WJ, Rabinstein AA, Ackerson T, et al.2018 guidelines for the early management of patients with acute ischemic stroke: a guideline for healthcare professionals from the American Heart Association/American Stroke Association. Stroke. 2018;49:e46–e99. [PubMed: 29367334]

15. Kidwell CS, Alger JR, Saver JLJS. Beyond mismatch: evolving paradigms in imaging the ischemic penumbra with multimodal magnetic resonance imaging. Stroke. 2003;34:2729–2735. [PubMed: 14576370]

16. Goyal M, Menon BK, Derdeyn CP. Perfusion imaging in acute ischemic stroke: let us improve the science before changing clinical practice. Radiology. 2013;266:16–21. [PubMed: 23264523]

17. Kuroiwa T, Nagaoka T, Ueki M, Yamada I, Miyasaka N, Akimoto H. Different apparent diffusion coefficient: water content correlations of gray and white matter during early ischemia. Stroke. 1998;29:859–865. [PubMed: 9550523]

18. Nicoli F, Lefur Y, Denis B, Ranjeva J, Confort-Gouny S, Cozzone P. Metabolic counterpart of decreased apparent diffusion coefficient during hyperacute ischemic stroke: a brain proton magnetic resonance spectroscopic imaging study. Stroke. 2003;34:e82–e87. [PubMed: 12817104]

19. Guadagno JV, Warburton EA, Jones PS, et al.How affected is oxygen metabolism in DWI lesions? A combined acute stroke PET-MR study. Neurology. 2006;67:824–829. [PubMed: 16966545]

20. Pierpaoli C, Alger JR, Righini A, et al.High temporal resolution diffusion MRI of global cerebral ischemia and reperfusion. J Cereb Blood Flow Metab. 1996;16:892–905. [PubMed: 8784233]

21. Beaulieu C, De Crespigny A, Tong DC, Moseley ME, Albers GW, Marks MP. Longitudinal magnetic resonance imaging study of perfusion and diffusion in stroke: evolution of lesion volume and correlation with clinical outcome. Ann Neurol. 1999;46:568–578. [PubMed: 10514093]

22. Ueda T, Yuh WT, Maley JE, Quets JP, Hahn PY, Magnotta VA. Outcome of acute ischemic lesions evaluated by diffusion and perfusion MR imaging. Am J Neuroradiol. 1999;20:983–989. [PubMed: 10445433]

23. Kidwell CS, Saver JL, Mattiello J, et al.Thrombolytic reversal of acute human cerebral ischemic injury shown by diffusion/perfusion magnetic resonance imaging. Ann Neurol. 2000;47:462–469. [PubMed: 10762157]

24. Merino JG, Latour LL, Todd JW, et al.Lesion volume change after treatment with tissue plasminogen activator can discriminate clinical responders from nonresponders. Stroke. 2007;38:2919–2923. [PubMed: 17901392]

25. Le Bihan DLooking into the functional architecture of the brain with diffusion MRI. Nat Rev Neurosci. 2003;4:469–480. [PubMed: 12778119]

26. Jensen JH, Helpern JA, Ramani A, Lu H, Kaczynski K. Diffusional kurtosis imaging: the quantification of non-gaussian water diffusion by means of magnetic resonance imaging. Magn Reson Med. 2005;53:1432–1440. [PubMed: 15906300]
27. Jensen JH, Falangola MF, Hu C, et al.Preliminary observations of increased diffusional kurtosis in human brain following recent cerebral infarction. NMR Biomed. 2011;24:452–457. [PubMed: 20960579]
28. Cheung JS, Wang E, Lo EH, Sun PZ. Stratification of heterogeneous diffusion MRI ischemic lesion with kurtosis imaging: evaluation of mean diffusion and kurtosis MRI mismatch in an animal model of transient focal ischemia. Stroke. 2012;43:2252–2254. [PubMed: 22773558]
29. Yin J, Sun H, Wang Z, Ni H, Shen W, Sun PZ. Diffusion kurtosis imaging of acute infarction: comparison with routine diffusion and follow-up MR imaging. Radiology. 2018;287:651–657. [PubMed: 29558293]
30. Baron CA, Kate M, Gioia L, et al.Reduction of diffusion-weighted imaging contrast of acute ischemic stroke at short diffusion times. Stroke. 2015;46:2136–2141. [PubMed: 26152297]
31. Lätt J, Nilsson M, van Westen D, Wirestam R, Ståhlberg F, Brockstedt S. Diffusion-weighted MRI measurements on stroke patients reveal water-exchange mechanisms in sub-acute ischaemic lesions. NMR Biomed. 2009;22:619–628. [PubMed: 19306340]
32. Klein S, Staring M, Murphy K, Viergever M, Pluim JP. Elastix: a toolbox for intensity-based medical image registration. IEEE Trans Med Imagingc. 2010;29:196–205.
33. Nilsson M, Szczepankiewicz F, van Westen D, Hansson O. Extrapolation-based references improve motion and eddy-current correction of high B-value DWI data: application in Parkinson's disease dementia. PLoS One. 2015;10:e0141825. [PubMed: 26528541]
34. Ning L, Nilsson M, Lasič S, Westin C-F, Rathi Y. Cumulant expansions for measuring water exchange using diffusion MRI. J Chem Phys. 2018;148:074109. [PubMed: 29471656]
35. Kärger JDiffusion Untersuchung von Wasser an 13X-sowie 4A-und 5A-Zeolithen mit Hilfe der Methode der gepulsten Feldgradienten. Z Phys Chem Leipzig. 1971;248:27–41.
36. Lasič S, Nilsson M, Lätt J, Ståhlberg F, Topgaard D. Apparent exchange rate mapping with diffusion MRI. Magn Reson Med. 2011;66:356–365. [PubMed: 21446037]
37. Nilsson M, Lätt J, van Westen D, et al.Noninvasive mapping of water diffusional exchange in the human brain using filter-exchange imaging. Magn Reson Med. 2013;69:1573–1581. [PubMed: 22837019]
38. Lasič S, Oredsson S, Partridge SC, et al.Apparent exchange rate for breast cancer characterization. NMR Biomed. 2016;29:631–639. [PubMed: 26929050]
39. Lampinen B, Szczepankiewicz F, Westen D, et al.Optimal experimental design for filter exchange imaging: apparent exchange rate measurements in the healthy brain and in intracranial tumors. Magn Reson Med. 2017;77:1104–1114. [PubMed: 26968557]
40. Nilsson M, Lätt J, Nordh E, Wirestam R, Ståhlberg F, Brockstedt S. On the effects of a varied diffusion time in vivo: is the diffusion in white matter restricted?Magn Reson Imaging. 2009;27:176–187. [PubMed: 18657924]
41. Lasič S, Szczepankiewicz F, Eriksson S, Nilsson M, Topgaard D. Microanisotropy imaging: quantification of microscopic diffusion anisotropy and orientational order parameter by diffusion MRI with magic-angle spinning of the q-vector. Front Phys. 2014;2:11.
42. Szczepankiewicz F, Lasič S, van Westen D, et al.Quantification of microscopic diffusion anisotropy disentangles effects of orientation dispersion from microstructure: applications in healthy volunteers and in brain tumors. Neuroimage. 2015;104:241–252. [PubMed: 25284306]
43. Szczepankiewicz F, van Westen D, Englund E, et al.The link between diffusion MRI and tumor heterogeneity: mapping cell eccentricity and density by diffusional variance decomposition (DIVIDE). Neuroimage. 2016;142:522–532. [PubMed: 27450666]
44. Nilsson M, Szczepankiewicz F, Brabec J, et al.Tensor-valued diffusion MRI in under 3 minutes: an initial survey of microscopic anisotropy and tissue heterogeneity in intracranial tumors. Magn Reson Med. 2020;83:608–620. [PubMed: 31517401]
45. Basser PJ, Mattiello J, LeBihan D. MR diffusion tensor spectroscopy and imaging. Biophys J. 1994;66:259. [PubMed: 8130344]

46. Inoue H, Okada Y. Roles of volume-sensitive chloride channel in excitotoxic neuronal injury. J Neurosci. 2007;27:1445–1455. [PubMed: 17287519]
47. Li P, Murphy TH. Two-photon imaging during prolonged middle cerebral artery occlusion in mice reveals recovery of dendritic structure after reperfusion. J Neurosci. 2008;28:11970–11979. [PubMed: 19005062]
48. Murphy TH, Li P, Betts K, Liu R. Two-photon imaging of stroke onset in vivo reveals that NMDA-receptor independent ischemic depolarization is the major cause of rapid reversible damage to dendrites and spines. J Neurosci. 2008;28:1756–1772. [PubMed: 18272696]
49. Budde MD, Frank JA. Neurite beading is sufficient to decrease the apparent diffusion coefficient after ischemic stroke. PNAS. 2010;107:14472–14477. [PubMed: 20660718]
50. Hossmann K-A. Pathophysiology and therapy of experimental stroke. Cell Mol Neurobiol. 2006;26:1055–1081.
51. Mukherjee P, Bahn MM, McKinstry RC, et al.Differences between gray matter and white matter water diffusion in stroke: diffusion-tensor MR imaging in 12 patients. Radiology. 2000;215:211–220. [PubMed: 10751489]
52. Fiehler J, Foth M, Kucinski T, et al.Severe ADC decreases do not predict irreversible tissue damage in humans. Stroke. 2002;33:79–86. [PubMed: 11779893]
53. Buja L, Eigenbrodt ML, Eigenbrodt EH. Apoptosis and necrosis. Basic types and mechanisms of cell death. Arch Pathol Lab Med. 1993;117:1208–1214. [PubMed: 8250690]
54. O'Brien MC, Healy SF, Raney SR, et al.Discrimination of late apoptotic/necrotic cells (type III) by flow cytometry in solid tumors. Cytom Part A. 1997;28:81–89.
55. Weerasinghe P, Hallock S, Brown RE, Loose DS, Buja LM. A model for cardiomyocyte cell death: insights into mechanisms of oncosis. Exp Mol Pathol. 2013;94:289–300. [PubMed: 22609242]
56. Schilling F, Ros S, Hu D-E, et al.MRI measurements of reporter-mediated increases in transmembrane water exchange enable detection of a gene reporter. Nat Biotechnol. 2017;35:75–80. [PubMed: 27918546]
57. Nilius BIs the volume-regulated anion channel VRAC a “water-permeable” channel?Neurochem Res. 2004;29:3–8. [PubMed: 14992260]
58. Mongin AA. Volume-regulated anion channel—a frenemy within the brain. Pflugers Arch - Eur J Physiol. 2016;468:421–441. [PubMed: 26620797]
59. Andersson JL, Skare S, Ashburner J. How to correct susceptibility distortions in spin-echo echo-planar images: application to diffusion tensor imaging. Neuroimage. 2003;20:870–888. [PubMed: 14568458]
60. Nilsson M, Szczepankiewicz F, Ahlgren A, et al.An open-source framework for analysis of multidimensional diffusion MRI data implemented in MATLAB. In: Proceedings of the 26th Annual Meeting of ISMRM, Paris, France, 2018. p 5355.
61. Brusini L, Menegaz G, Nilsson M. Monte Carlo simulations of water exchange through myelin wraps: implications for diffusion MRI. IEEE Trans Med Imaging. 2019;38:1438–1445. [PubMed: 30835213]
62. Jin J-F, Guo Z-T, Zhang Y-P, Chen Y-Y. Prediction of motor recovery after ischemic stroke using diffusion tensor imaging: a meta-analysis. World J Emerg Med. 2017;8:99. [PubMed: 28458752]
63. Szczepankiewicz F, Hoge S, Westin C-F. Linear, planar and spherical tensor-valued diffusion MRI data by free waveform encoding in healthy brain, water, oil and liquid crystals. Data Brief. 2019;25:104208. [PubMed: 31338402]
64. Lustig M, Donoho D, Pauly JM. Sparse MRI: the application of compressed sensing for rapid MR imaging. Magn Reson Med. 2007;58:1182–1195. [PubMed: 17969013]
65. Veraart J, Fieremans E, Novikov DS. Diffusion MRI noise mapping using random matrix theory. Magn Reson Med. 2016;76:1582–1593. [PubMed: 26599599]
66. Plenge E, Poot DH, Bernsen M, et al.Super-resolution methods in MRI: can they improve the trade-off between resolution, signal-to-noise ratio, and acquisition time?Magn Reson Med. 2012;68:1983–1993. [PubMed: 22298247]
67. Nilsson M, Westin C-F, Brabec J, Lasic S, Szczepankiewicz F. A unified framework for analysis of time-dependent diffusion: numerical validation of a restriction-exchange correlation experiment. In: Proceedings of the Virtual Conference of ISMRM and SMRT, 2020. Abstract #p 718.

68. Jensen JH, Helpern JA. Effect of gradient pulse duration on MRI estimation of the diffusional kurtosis for a two-compartment exchange model. J Magn Reson. 2011;210:233–237. [PubMed: 21459638]

69. Nilsson M, Szczepankiewicz F, Ahlgren A, et al.An open-source framework for analysis of multidimensional diffusion MRI data implemented in MATLAB. In: Proceedings of the 26th Annual Meeting of ISMRM, Paris, France, 2018. p 5355.

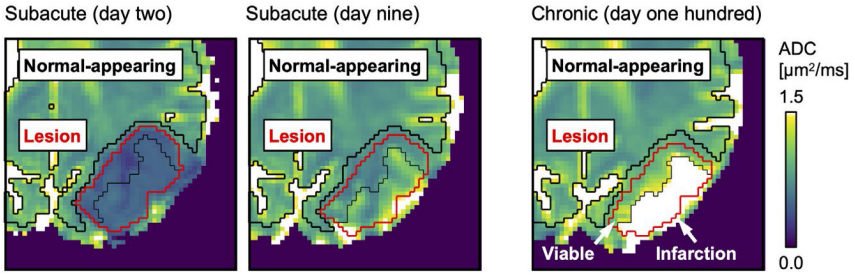

FIGURE 1.

The stroke lesions were manually defined based on ADC reduction on day 2 after stroke onset (red region of interest [ROI]). The thin black line separates tissue that, by day 100, would either be infarcted (ADC > 1.2 μm^2/ms) or remain viable (ADC ≤ 1.2 μm^2/ms; arrows). The lesion definitions were made on spatially aligned ADC maps and were applied to all time points, with small manual corrections. Normal-appearing tissue was defined as non-lesion voxels with ADC ≤ 1.2 μm^2/ms (thick black ROI)

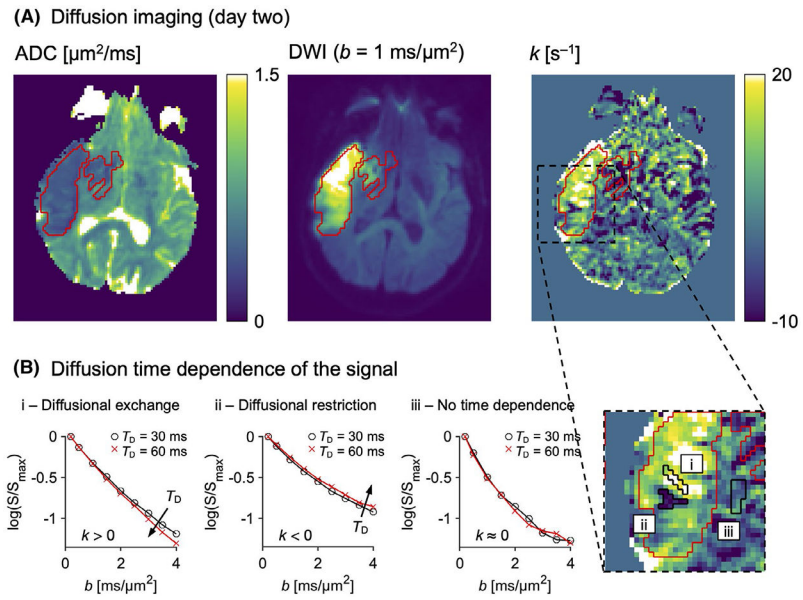

FIGURE 2.

Diffusion time dependence in ischemic stroke. A, The same stroke lesion (red ROI) is shown on an ADC map, a diffusion-weighted image (DWI), and a rate of kurtosis change (*k*) map. The lesion was evident in the *k* map, exhibiting large regions with elevated values. B, The values of *k* reflected a diffusion time (T_D) dependence of the signal, as illustrated for tissue within small black ROIs on a magnified part of the *k* map. Regions with positive *k* covered most of the lesion (i), reflecting a decreased signal curvature with longer T_D and indicating diffusional exchange. Small regions with negative *k* were also seen (ii), reflecting the opposite signal pattern and indicating restricted diffusion. Most normal-appearing tissue featured a *k* near zero (iii), indicating no diffusion time dependence

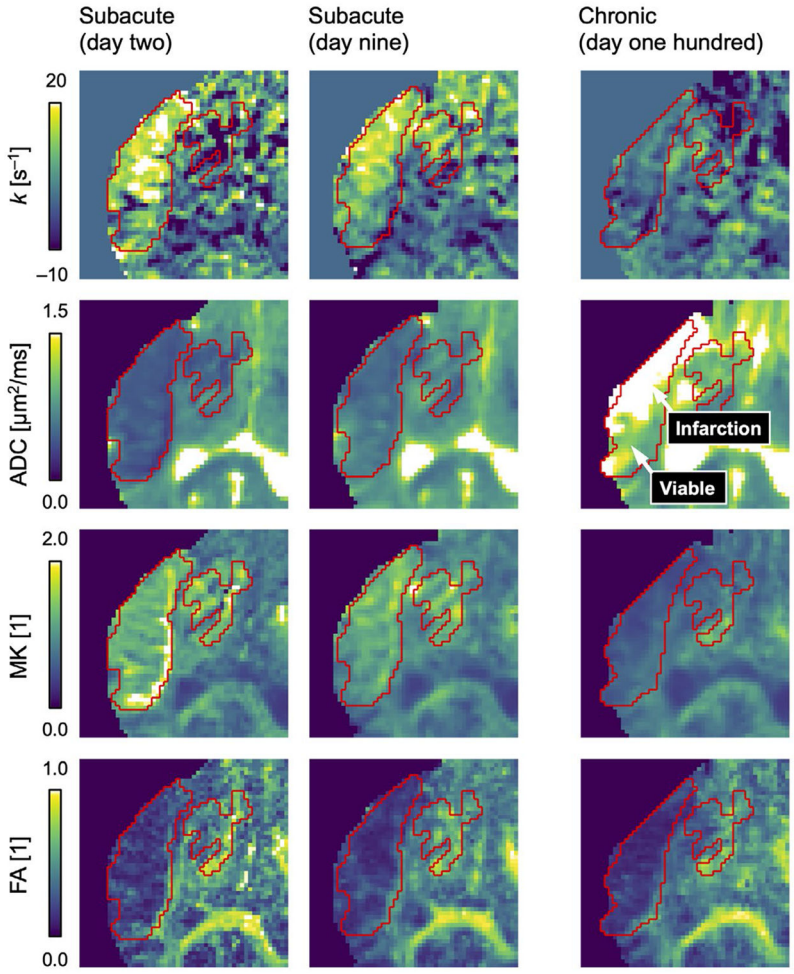

FIGURE 3.

Progression of diffusion parameter maps in ischemic stroke. The rate of kurtosis change (*k*) was elevated within lesions (red ROIs) compared with normal-appearing tissue on day 2 (Table 2; $P = .001$) and day 9 ($P = .023$), indicating diffusional exchange. The ADC was pseudo-normalized on day 9. On day 100, a heterogeneous pattern of elevated ADC indicated infarction within 50 ± 20% of the original lesion volumes. The mean kurtosis (MK) progressed from elevated on day 2, through pseudo-normalized on day 9, to reduced on day 100. The fractional anisotropy (FA) was reduced at all time points

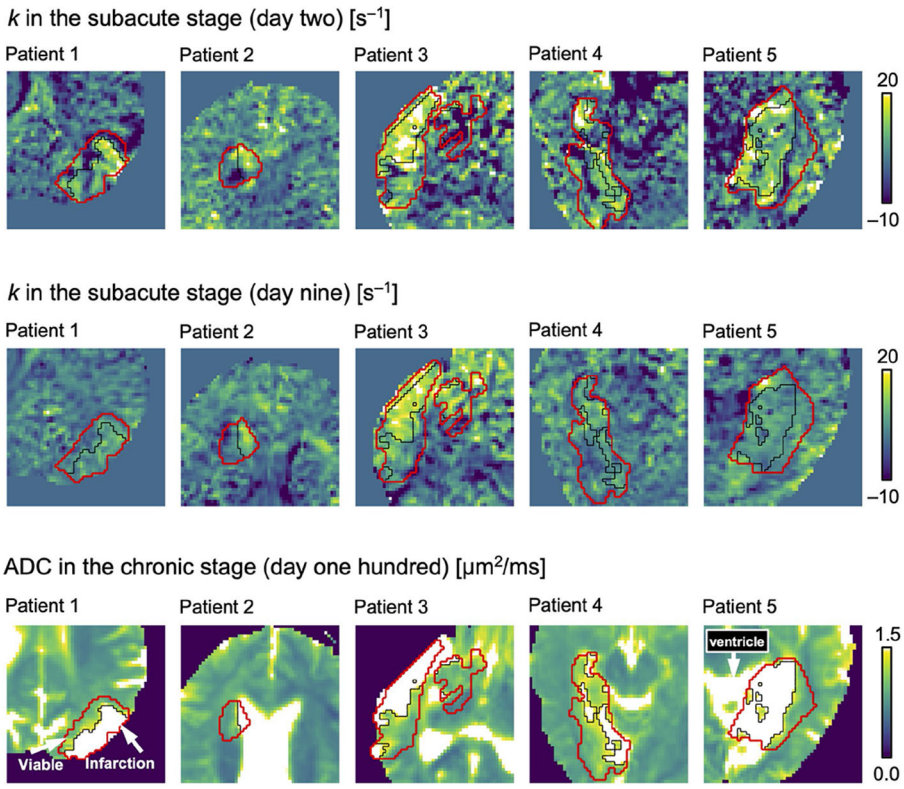

FIGURE 4.

Diffusion time dependence versus tissue outcome. The red ROIs indicate the stroke lesions, and thin black lines divide the lesions between tissue that, by day 100, would either be infarcted (ADC > 1.2 μm^2/ms) or remain viable (ADC ≤ 1.2 μm^2/ms; arrows). The pattern of the rate of kurtosis change (k) at the subacute stage was similar to the pattern of infarction at the chronic stage. The value of k was higher in tissue that would be infarcted than in tissue that would remain viable both on day 2 (Table 3; P = .026) and on day 9 (P = .046), indicating a relationship between elevated rates of water exchange and eventual tissue infarction. Note that for patients 2 and 5, the ADC within the liquid part of the lesion on day 100 was similar to in the ventricles, making them appear confluent

TABLE 1

Patient and lesion characteristics

Patient			Time point (days)			Lesion			
No.	**Sex**	**Age (years)**	**Exam 1**	**Exam 2**	**Exam 3**	**Size[a] (mL)**	**Side**	**Location**	**Occluded vessel**
1	F	50	3	11	114	22	Left	PL	MCA[b]
2	F	45	2	8	107	10	Right	BG	MCA[c]
3	M	52	1	8	95	43	Right	TL, BG	MCA[d]
4	F	31	4	10	104	32	Right	OL, HC	PCA
5	M	59	2	8	133	62	Left	OL, HC	PCA
		47 (10)	2 (1)	9 (1)	111 (14)	34 (20)			

Note: The last row shows the mean (SD) for the numerical data.

Abbreviations: BG, basal ganglia; F, female; HC, hippocampus; M, male; MCA, middle cerebral artery; OL, occipital lobe; PCA, posterior cerebral artery; PL, parietal lobe; TL, temporal lobe.

[a]The volume of ADC reduction at exam 1. Note that the acquisition lacked full spatial coverage of all lesions.

[b]Posterior branch.

[c]Lenticulostriate perforants.

[d]Anterior branch and lenticulostriate perforants.

TABLE 2

Progression of diffusion parameters in ischemic stroke

Parameter	Time point	Lesion	N-A	*P*-Value
k [s^{-1}]	Day 2	6.0 (1.2)	2.5 (0.8)	.001
	Day 9	5.0 (1.5)	2.0 (1.3)	.023
	Day 100	−0.6 (1.4)	2.0 (1.8)	.073
ADC [μm^2/ms]	Day 2	0.52 (0.11)	0.85 (0.03)	.002
	Day 9	0.81 (0.15)	0.87 (0.03)	.406
	Day 100	1.53 (0.20)	0.89 (0.04)	.002
MK [1]	Day 2	1.19 (0.15)	0.79 (0.06)	.004
	Day 9	0.94 (0.18)	0.78 (0.04)	.079
	Day 100	0.61 (0.08)	0.79 (0.03)	.003
FA [1]	Day 2	0.26 (0.05)	0.37 (0.02)	.010
	Day 9	0.26 (0.05)	0.35 (0.02)	.002
	Day 100	0.25 (0.08)	0.37 (0.03)	.005

Note: Data are shown as mean (SD) across the 5 patients.

Abbreviation: N-A, normal-appearing tissue.

TABLE 3

Diffusion parameters versus tissue outcome in ischemic stroke

Parameter	Time point	Infarcted	Viable	*P*-Value
k [s^{-1}]	Day 2	9.5 (3.1)	3.6 (3.0)	.026
	Day 9	7.2 (3.4)	3.6 (1.0)	.046
ADC [μm^2/ms]	Day 2	0.54 (0.13)	0.50 (0.07)	.204
	Day 9	0.87 (0.20)	0.75 (0.11)	.077
MK [1]	Day 2	1.14 (0.16)	1.24 (0.14)	.043
	Day 9	0.91 (0.22)	0.97 (0.14)	.235
FA [1]	Day 2	0.21 (0.05)	0.31 (0.07)	.059
	Day 9	0.20 (0.05)	0.31 (0.06)	.029

Note: Data are shown as mean (SD) across the 5 patients.